Accepted Version: Chen, Y., D. Tyagi, M. Lu, A. Carrier, C. Nganou, B. Youden, W. Wang, S. Cui, M. Servos, K. Oakes, S. He, X. Zhang. 2019. A regenerative NanoOctopus based on multivalent-aptamer functionalized magnetic microparticles for effective cell capture in whole blood. Analytical Chemistry 91(6):4017–4022. http://doi.org/10.1021/acs.analchem.8b05432

A regenerative NanoOctopus based on multivalent-aptamer functionalized magnetic microparticles for effective cell capture in whole blood

Yongli Chen,[a‡] Deependra Tyagi,[b‡] Mingsheng Lu,[b,c] Andrew J. Carrier,[b] Collins Nganou,[b] Brian Youden,[b,d] Wei Wang,[e] Shufen Cui,[f] Mark Servos,[d] Ken Oakes,[g] Shengnan He,*[e] and Xu Zhang*[b]

[a]Postdoctoral Innovation Practice Base, Shenzhen Polytechnic, Shenzhen, 518055, China. [b]Verschuren Centre for Sustainability in Energy and the Environment, Cape Breton University, 1250 Grand Lake Road, Sydney, Nova Scotia, B1P 6L2, Canada. [c]Marine School, Huaihai Institute of Technology, Lianungang, 222005, China. [d]Department of Biology, University of Waterloo, Waterloo, Ontario, N2L 3G1, Canada. [e]Institute of Translational Medicine, Shenzhen Second People's Hospital, First Affiliated Hospital of Shenzhen University, Health Science Center, Shenzhen, 518055, China. [f]Department of Biological Applied Engineering, Shenzhen Key Laboratory of Fermentation, Purification and Analysis, Shenzhen Polytechnic, Shenzhen, 518055, China. [g]Department of Biology, Cape Breton University, 1250 Grand Lake Road, Sydney, Nova Scotia, B1P 6L2, Canada.

KEYWORDS Multivalent aptamer, cell isolation, circulating tumor cells, cancer diagnosis

ABSTRACT: Isolation of specific rare cell subtypes from whole blood is critical in cellular analysis and important in basic and clinical research. Traditional immuno-magnetic cell capture suffers from suboptimal sensitivity, specificity, and time- and cost-effectiveness. Mimicking the features of octopuses, NanoOctopus devices were developed for cancer cell isolation in whole blood. The device consists of long multimerized aptamer DNA strands, or tentacle DNA, immobilized on magnetic microparticle surfaces. Their ultrahigh sensitivity and specificity are attributed to multivalent binding of the tentacle DNA to cell receptors without steric hindrance. The simple, quick, and non-invasive capture and release of the target cells allows for extensive downstream cellular and molecular analysis and the time- and cost-effectiveness of fabrication and regeneration of the devices makes them attractive for industrial manufacture.

Isolation of specific cell subtypes from biological fluids is the first step in cellular analysis, which is important in basic and clinical research of complex diseases, such as cancer. High cellular heterogeneity leads to challenges in accurate analysis, affecting diagnostics and personalized treatment.[1] For cancer diagnosis and prognosis, circulating tumor cells (CTCs) are "liquid biopsies" as CTCs contain all the real-time molecular information for tumor development and metastasis during sampling.[2–4]

Currently, target cell separations are based on their size,[5] surface adhesivity,[6] or unique marker proteins on cell surfaces[7] that can be specifically recognized by affinity ligands, such as antibodies,[8] peptides,[9] or aptamers.[9,10] Although microfluidics[11–15] and nanomaterials[16–20] are widely used for methodology development, resulting in significant advancements, most of these methods remain suboptimal considering their efficiency, invasiveness, and time- and cost- effectiveness.[21–23]

By mimicking the structure of octopuses that use long tentacles, each containing many suckers for efficient capture of prey in a "multivalent" manner,[11,24,25] we developed NanoOctopus devices for cell capture in blood (Scheme 1). The NanoOctopuses are comprised of a magnetic microparticle (MP) mimicking the octopus head and long single stranded DNA sequences anchored on the MP surface as tentacles. Each DNA sequence contains >500 repeating "suckers" of DNA aptamer sequences that specifically bind target biomarker proteins on cell membranes. Cell separation using long multimerized aptamer

(Multi-A) DNAs was originally demonstrated in a microfluidic chip by Zhao et al.,[11] where the Multi-A-DNAs were immobilized on microfluidic channels forming 3D networks with improved efficiency in cell isolation at high flow rates, in contrast to those microfluidic devices using single-unit aptamer or antibody functionalized surfaces.[11] Although this chip design is creative and inspiring, its sensitivity is still not optimal because cell capture requires diffusion of cells towards the channel walls to be captured by the DNA network, whereas at high flow rates the DNA networks are pushed against the microchannel walls while majority of cells tend to quickly travel through the middle of the channel thus reducing the probability of capture. Additionally, its practical application is limited because of its complex fabrication process. The need for syringe pumps and electricity restricts its point-of-care (POC) application, especially in remote and resource-limited areas. These issues have been addressed by NanoOctopus devices, which can diffuse throughout the sample medium, and thus can actively capture the target cells, resulting in superior performance for cell isolation in whole blood.

NanoOctopus fabrication is straightforward (Scheme 1A). First, biotinylated 20A sequences (see SI) were immobilized on streptavidin-functionalized MPs (diameter 4 μm) via specific biotin-streptavidin binding to anchor the tentacle DNA sequences. The tentacles are long DNA strands (≥40 000 nucleotides) prepared via rolling circle amplification (RCA) performed at 25 ºC for 10 min (Fig. S1).[26–28] Each tentacle DNA contains 100s to 1000s of repeating aptamer units spaced by 20T sequences. The spacers minimize aptamer misfolding, maximizing the capture capacity and provide many anchoring sites to be assembled with the MPs via a 5-min hybridization with the 20A anchor DNA.[11] The assembly effectiveness is demonstrated in Fig. S2, where most MPs were covered by FAM-stained tentacle DNA. The tentacle DNA interacted with the MP surface indirectly, minimizing steric hindrance. In contrast, directly growing tentacle DNA on MP surfaces was unsuccessful, resulting in ineffective NanoOctopuses (data not shown), likely because of steric hindrance affecting RCA and misfolding of the aptamer units within the tentacle DNA.

NanoOctopuses were tested for cell isolation and CCRF-CEM cells from a human acute lymphoblastic leukemia (AML) cell line (CCL-119 T-cell), were used as the test model.[29,30] The concentration and molecular subtypes of CCRF-CEM cells in peripheral blood are useful for AML diagnosis and prognosis.[31,32] CCRF-CEM cells express protein tyrosine kinase 7 (PTK7),[33] a membrane marker protein that is specifically recognized by the DNA aptamer selected by Tan et al.[34] In contrast, PTK7 expression in Ramos (RA 1) cells, which were used as the control, is low (Fig. S3). Tentacle DNA and the NanoOctopus binding (Fig. S4) towards the CCRF-CEM cells was confirmed by fluorescence microscopy. Instances of multiple cells captured by one NanoOctopus and vice versa were observed, indicating the multivalent binding capability of the NanoOctopuses (Fig. S5).

The efficiency and selectivity was demonstrated by retrieving CCRF-CEM cells (2000/mL, stained with the green fluorescence dye, DIO) from a cell mixture in phosphate buffered saline (PBS, pH 7.4) containing RA 1 cells (at a ratio of either 1:1 or 2:1 to CCRF-CEM cells) or regular white blood cells (WBCs, 10^7/mL, separated from 1 mL of whole blood and stained with the red fluorescence dye, DID). As shown in Fig. 1A, although the number of non-specifically captured RA 1 cells slightly increased when twice the number of RA 1 cells were in the system, the CCRF cell capture efficiency remained ~95%. Similarly, the capture efficiency (88±6%) and purity (96.7%) of the target cells were superior in the presence of WBCs (at 5000 times the CCRF-CEM cell concentration) in PBS buffer and whole blood (Figs. 1C and D). Compared with an established aptamer-based magnetic cell separation method where MPs were functionalized with single-unit aptamer molecules (MP-UA), the NanoOctopuses dramatically improved the capture efficiency and purity in both PBS and whole blood (Figs. 1C and D). The data show that the MP-UA devices were incapable of isolating target cells at low concentrations, *e.g.,* 25 cells/mL, from either PBS or whole blood. However, the NanoOctopuses captured target CCRF cells even when their concentration was only 1–10 cells/mL in whole blood, with capture efficiencies of ~35% and ~20% when the spiked target cell concentrations were 10 and 1 cell(s)/mL, respectively (Figs. S6 and S7). If cancer cells are in patient blood at a concentration of 1 cell/mL, the NanoOctopuses should capture them from 5–10 mL blood samples; therefore, the results demonstrated sufficient sensitivity of the NanoOctopuses for CTC isolation and sample-preparation for single-cell analysis.

The cell capture purity (the percentage of target cells in the total number of captured cells) by NanoOctopuses was affected by the capture efficiency, especially when the target cell concentrations were low (Fig. 1D). As shown in Fig. S5B, some WBCs (red fluorescence) were also captured with CCRF-CME cells (green fluorescence). These WBCs were considered as an "impurity"; however, considering WBC heterogeneity, a small number of WBCs, similar to RA 1 cells (Fig S3), may express PTK7, which was confirmed experimentally (Fig. S8). Therefore, if all PTK7 expressing cells are considered target cells, the cell capture purity is high, further demonstrating the effectiveness of the method.

Three mechanisms lead to the high NanoOctopus capture efficiency. First, multivalent binding improves the binding avidity of the multimeric aptamer towards the target cells.[11,24,25,35–37] After 4 rinsing steps only ~3% of captured CCRF cells were rinsed off the NanoOctopuses while 95% were retained. In contrast, 33–50% of the CCRF cells captured by MP-UA devices were lost after 2–4 rinses (Fig. S9a); thus, lower binding avidity resulted in lower capture efficiency after multiple rinses, which are required to improve the target cell purity by removing non-specifically bound cells (Fig. S9B). Second, the long tentacle DNA strands increase the effective size of NanoOctopuses, improving the aptamer accessibility to cell receptors and their collision probability, resulting in more efficient binding, especially when the target cell concentration is very low (*i.e.,* ≤10 cells/mL in whole blood; the hydrodynamic diameter of the NanoOctopuses made with 1 μm MPs is 6.361±0.262 μm in PBS, while that for the MP-UA devices is 1.054±0.042 μm). Additionally, the tentacle DNA length (~2.7 μm) decreased steric hindrance from the particle surfaces and ensured high capture efficiency, which was substantiated by quantitative analysis of the number of DNA strands on each MP. For MP-UA devices, there were ~5.7×10^4 unit aptamers immobilized on each MP, while ~2350 tentacle DNA strands, i.e., RCA products (equivalent to 7.0×10^5 unit aptamers, based on DNA length shown in Fig S1) were attached on each MP to form a NanoOctopus device. Notably, the higher surface density of the unit aptamers on the MP surface (~24 times of the tentacle DNA) did not lead to higher binding

avidity to cells, indicating the critical effect of the steric hindrance on the cell capture, which confirmed that engineering the NanoOctopus device free of steric hindrance is an innovative and promising approach to achieve highly effective cell capture. Finally, the long NanoOctopus tentacles allow for using larger MPs (4 μm) with strong magnetic responsiveness to external fields, allowing for higher recovery of large MPs via magnetic separation in a short time (10 min), improving sample throughput.

We used irreversible bimolecular reaction kinetics to model NanoOctopus cell-capture (see SI) to determine the effect of the physicochemical properties of NanoOctopuses on cell capture kinetics. Multiple interactions between the NanoOctopuses and target cells were ignored because a single NanoOctopus-cell interaction is the first step in cell capture even in multiple binding situations. The mathematical model (Eq. 1) describes how experimental factors, including sample volume (V_{sample}), capture time (t), effective size, mass transfer coefficients (D_{cell} and D_{MP}), and concentrations of the NanoOctopuses ([MP]) and target cells ([$cell$]), collectively determine the number of target cells (n) being captured.

$$n = 4\pi(D_{cell} + D_{MP})(r_{cell} + r_{MP})[cell][MP]V_{sample}t \qquad (1)$$

Herein, we use the mass transfer coefficients, D_{cell} and D_{MP}, similar to diffusivity, to describe the cell and MP mobility in samples mildly agitated by a horizontal shaker. The mass transfer coefficients are governed by shaker speed, but are inversely proportional to particle size and medium viscosity.[38–40] The hydrodynamic radii of the target cell (r_{cell}) and NanoOctopus (r_{MP}) measured by dynamic light scattering were used to represent their encounter radii. Based on the excellent experimental data fit (Fig. 1C), the model can interpret the data and guide experimental design, *e.g.,* when the target cell concentration is low, extending the capture time and increasing the NanoOctopus concentration may improve cell capture (Fig. S10 and S11).

Similarly, cell capture by MP-UAs was modelled using reversible bimolecular reaction kinetics (Eq. 13 in SI). The lack of multivalent cell-binding capability of the MP-UA results in low binding avidity and reversible cell binding, as supported by rinsing experiments (Fig. S9A). Additionally, their small size, the steric hindrance of the MP against the unit aptamers, and the small distance between cells and MPs collectively contributed to their lower capture efficiency and sensitivity.

Non-invasiveness of the cell capture and release procedure is critical to ensure the viability of captured CTCs for further analysis. First, the cell release procedure is mild and simple. A 20 min DNase treatment at 37 ºC degrades the tentacle DNA and the MPs are removed magnetically, releasing most captured cells (87.7±3.5%, Scheme 1B). Second, no NanoOctopus endocytosis was observed, in contrast with significant uptake of the MP-UAs during 1 h incubation (Fig S12). The endocytosis of particles functionalized with short DNA strands, *i.e.,* aptamer and siRNA functionalized nanoparticles, is a delivery tool for drugs and genes or for diagnostics.[41] However, the large size (2.7 μm) of tentacle DNAs protected NanoOctopuses from cellular uptake.[42] Although internalized particles may not immediately kill cells, potential damage is possible, *e.g.,* metal oxide nanoparticles released from degraded MPs can induce oxidative stress via reactive oxygen species generation.[43] Third, the proliferation capability of the recovered cells was confirmed by a 3 d cell culture experiment (Fig. S13) with no significant difference (p<0.05) compared to control cells (CCRF cells without cell-isolation treatment). After further culture for 7 d, 94% of the recovered cells remained viable, with no significant difference (p>0.05) from the control (99%).

The NanoOctopus device is regenerative, which improves its cost-effectiveness. Using locked nucleic acid (LNA)-based anchor sequences to immobilize the tentacle DNA on MP surfaces allows the NanoOctopus devices to be regenerated. The LNA sequence improved the duplex stability and hybridization specificity with the 20T-spacers in the tentacle DNA to form stable NanoOctopuses and increased the anchor DNA resistance to DNase degradation.[44,45] Fig. S14 shows a <18% decrease in cell capture efficiency of the same batch of MP-anchor DNA composite after 8 uses. Nevertheless, the <3% loss of capture efficiency for each additional use of the NanoOctopuses can be easily addressed by supplementing an additional 3% freshly prepared material. In addition, there was no loss of capture efficiency using freeze-dried MP-anchor DNA composites to regenerate the NanoOctopuses (Fig S15), offering great convenience for transportation and storage, and enhancing the potential for POC applications.

To demonstrate the clinical potential of the technique, the NanoOctopuses were applied to whole blood from 33 AML patients and 5 healthy donors as control. PTK7-expressing cancer cells were successfully (100% detection) isolated from a small volume of whole blood (0.5 –1 mL for each sample, Fig. 2) in all patient's blood while no such cells were detected in blood samples from healthy donors. Validation was performed by fluorescent antibody staining, showing negative for leukocyte marker CD 45 but positive for PTK7. Therefore, the NanoOctopus devices offer a promising tool for rare cell isolation from whole blood.

A striking advantage of the NanoOctopus device is its translational potential for commercialization. The device is novel in its concept and design, organically combining the powerful binding avidity of the Multi-A DNAs with the mobility and simple separation of MPs in an external magnetic field, thus demonstrating excellent performance. However, its fabrication is based on well-established components and techniques. For example, the avidin-functionalized MNPs and biotinylated anchor DNAs are commercially available; the RCA technique and DNA attachment onto nanosurfaces via hybridization are well established, which thus guarantee the robustness and cost-effectiveness of device manufacture. In addition, magnetic separation suits automated and high-throughput operation using 96-well plates and commercial systems, such as the KingFisher purification system from Thermo Scientific and MagNA Pure 96 system from Roche Diagnostics USA, which would facilitate large-scale sample treatment in parallel.

CONCLUSIONS

NanoOctopus devices efficiently and selectively isolate target cells from complex mixtures, including whole blood. Single cell isolation is possible, allowing for the sensitive detection of circulating tumor cells from small blood samples. Many of the benefits of NanoOctopuses derive from their irreversible and unhindered multivalent binding of target cells, but they are also non-invasive, resisting endocytosis and being readily removed through degradation of binding DNA aptamer strands. This allows for target cells to be cultured and the NanoOctopuses to be reused.

EXPERIMENTAL

Details of the material and methods used, and the mathematical modelling of the data are given in the Supporting Information. Herein are the experimental procedures required to facilitate understanding and reproduction of the results and discussion.

Fabrication of NanoOctopus devices

The NanoOctopus devices consist of long tentacle DNAs immobilized on anchor DNA (20A) functionalized MPs via DNA hybridization. Long tentacle DNAs that bind the PTK7 receptor were prepared using a rolling circle amplification (RCA) reaction, following the reported procedure with slight modification.[46] The method consists of two steps: first, circular DNA was prepared by annealing the circular RCA template and ligating with the ligation primer. Second, the prepared circularized DNA was used to perform the final RCA reaction. The final RCA product was characterized with 1% agarose gel electrophoresis and imaged on a blue-light transilluminator. DNA purification was performed using the phenol/chloroform method and the concentration of circularized DNA and the RCA product were determined by UV-Vis spectroscopy. To prepare the anchor DNA (biotin-labeled 20A) functionalized MPs, the avidin-coated MNPs were suspended in PBS buffer (pH 7.4) were mixed with an excess amount of anchor DNA (the molar ratio of anchor DNA and particles was 4.8×10^5:1) for overnight incubation at ambient temperature. Afterwards, the anchor DNA-MP complexes were collected by magnetic separation and the free anchor DNAs were washed away with PBS. To assemble the NanoOctopus devices, first, the PTK7 RCA products were denatured for 5 min at 95 ºC and then quickly cooled on ice for 10 min to minimize unwanted secondary structures. Second, streptavidin-coated MPs were incubated together with the PTK7 RCA products on a horizontal shaker (200 rpm) overnight at ambient temperature. The NanoOctopuses were separated magnetically with a magnetic stand and then rinsed twice with PBS to remove the free RCA product. For comparison, unit aptamer functionalized MPs were prepared in the same way. Afterwards, the NanoOctopuses and MP-unit aptamer complexes were characterized using a Zetasizer Nano ZS90 (Malvern Instruments, Southborough, UK) for their hydrodynamic sizes and surface charges (Fig. S16).

Application of NanoOctopus device for cancer cell separation

CCRF-CEM and Ramos cells were cultured in RPMI 1640 medium supplemented with 10% FBS in a humidified incubator at 37 ºC containing 5% CO_2. Before cell capture experiments, CCRF-CEM cells were stained with DIO, and Ramos cells (background cells) were stained with DID at 37 ºC for 10 min. The cells were rinsed with PBS buffer, resuspended, and stored on ice until further dilution to the desired concentration for use. To evaluate the cell capture efficiency and purity, DIO-stained CCRF-CEM cells were diluted to different concentrations and spiked in either simulated blood or PBS. The synthetic whole blood was prepared in four steps. First, WBCs were fractionated from healthy blood samples (EDTA-anticoagulated) using a density gradient centrifugation in Histopaque Ficoll medium following the reported method.[47] Second, the separated WBCs (background cells) were incubated with DID dye at 37 ºC for 10 min for staining. Third, to prepare whole blood matrix without WBCs, after a centrifugation treatment (1000 rpm, 5 min) of the whole blood to precipitate the WBCs, the supernatant, i.e., the whole blood matrix, was transferred to a fresh EDTA-anticoagulated microtube for storage. Finally, the DID-stained WBCs were added into the whole blood matrix with the final concentration of 1×10^7 cells mL^{-1} to obtain the synthetic whole blood, which was used to simulate whole blood. For target cell separation, 100 µL of the NanoOctopus solution was incubated with the cells (including defined concentrations of stained target cells and background cells) either in PBS or EDTA-anticoagulated synthetic blood for 30 min at ambient temperature. The resulting solutions were separated using a magnetic stand and washed twice with PBS. To release the captured cells from the NanoOctopuses, DNase I was introduced into the captured cell solution to degrade the tentacle DNAs. After separation using a magnetic stand, the released cells were collected to further test their proliferation and viability, while the anchor-DNA-MP complexes were collected to test their reusability and regenerative capacity.

Cell enumeration method

To enumerate a very small number of cells, e.g., <10 cells in buffer, neither conventional hematimetry nor flow cytometry were accurate enough or convenient to use. Therefore, a simple rare cell enumeration microchip was fabricated (detailed in the Supporting Information), which possesses open microwells within a PDMS membrane covered glass slide. When the cell concentrations were >1000 cells mL^{-1}, they were counted using a FACS Calibur flow cytometer (Becton Dickinson, CA, USA).

Application for clinical blood samples from AML patients

Thirty-three fresh whole-blood samples from leukemia patients and 5 blood samples from healthy donors (contained in EDTA-anticoagulated micro-tubes) were provided by Shenzhen Second People's Hospital (Protocol # 2018-03-16 with Institutional approval by the Hospital Review Board). After the NanoOctopus solution was mixed with undiluted blood samples (1 mL) and incubated for 1 h at ambient temperature, the captured cells were separated magnetically and rinsed with PBS. Afterwards, cell counting, immunostaining, and confocal imaging were performed to enumerate and validate the separated PTK7-expressing leukemia cells.

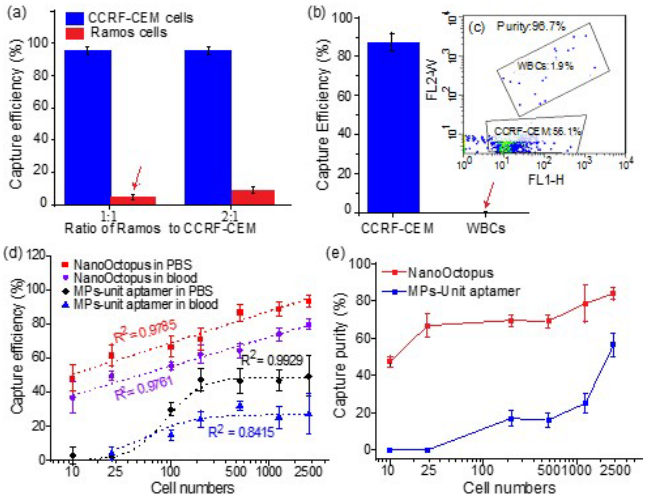

Figure 1. The capture efficiencies of NanoOctopuses for CCRF-CEM cells from PBS buffer samples containing (a) Ramos cells at various ratios and (b) 1.0 X 10^7 white blood cells. Inset: the purity of the captured cells determined by flow cytometry. (c) Capture efficiencies as a function of the target cell concentrations in PBS and whole blood (dashed lines showing the fit of the data with the mathematical models in SI). (d) Purity of the cells isolated from whole

blood samples as a function of the target cell concentrations for NanoOctopuses and single aptamer functionalized magnetic particles. Error bars represent the standard deviation for n=3.

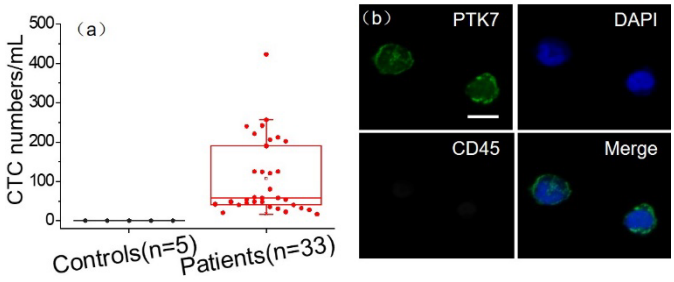

Figure 2. (a) Isolation of CCRF cells from the whole blood (0.5 – 1.0 mL /sample) collected from 33 acute lymphoblastic leukemia (AML) patients using NanoOctopuses. (b) Validation by confocal microscopic imaging with both fluorescence-labelled antibodies targeting CD 45 and PTK7 receptors (Scale bar: 10 μm).

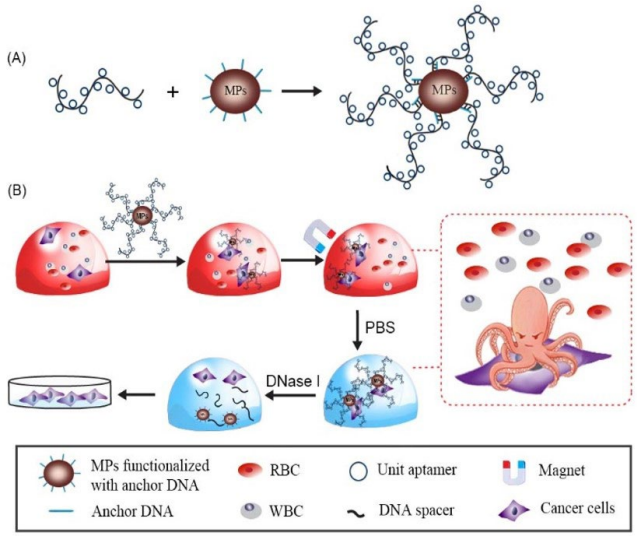

Scheme 1. Fabrication and Application of NanoOctopus Devices.

(A) Design and fabrication of the NanoOctopus device and (B) target cell capture from whole blood sample and release for downstream analysis.

ASSOCIATED CONTENT

Supporting Information

Experimental procedures, mathematical modelling, and supporting figures.

The Supporting Information is available free of charge on the ACS Publications website.

Supporting information (PDF)

AUTHOR INFORMATION

Corresponding Author

* S. H. E-mail: eheshengnan@163.com and X. Z. E-mail: Xu_Zhang@cbu.ca.

Author Contributions

All authors have given approval to the final version of the manuscript. ‡These authors contributed equally.

ACKNOWLEDGMENT

This work was supported by Beatrice Hunter Cancer Research Institute (BHCRI), Guangdong Province Higher Vocational College & School's Pearl River Scholar Funded Scheme (2017), National Natural Science Foundation of China (No. 21602138), Natural Science Foundation of Guangdong Province (No. 2016A030310032), the Atlantic Canada Opportunities Agency AIF program, Cape Breton University RISE program, and NSERC Discovery Grants Program.

REFERENCES

(1) Navin, N.; Kendall, J.; Troge, J.; Andrews, P.; Rodgers, L.; McIndoo, J.; Cook, K.; Stepansky, A.; Levy, D.; Esposito, D.; Muthuswamy, L.; Krasnitz, A.; McCombie, W. R.; Hicks, J.; Wigler, M. *Nature* **2011**, *472*, 90-94.

(2) Shen, Z.; Wu, A.; Chen, X. *Chem Soc Rev* **2017**, *46*, 2038-2056.

(3) Siravegna, G.; Marsoni, S.; Siena, S.; Bardelli, A. *Nat Rev Clin Oncol* **2017**, *14*, 531-548.

(4) Hong, S.; Wang, A. Z. *Adv Drug Deliv Rev* **2018**, *125*, 1-2.

(5) Hao, S. J.; Wan, Y.; Xia, Y. Q.; Zou, X.; Zheng, S. Y. *Adv Drug Deliv Rev* **2018**, *125*, 3-20.

(6) Myung, J. H.; Gajjar, K. A.; Saric, J.; Eddington, D. T.; Hong, S. *Angew Chem Int Ed Engl* **2011**, *50*, 11769-11772.

(7) Punnoose, E. A.; Atwal, S. K.; Spoerke, J. M.; Savage, H.; Pandita, A.; Yeh, R. F.; Pirzkall, A.; Fine, B. M.; Amler, L. C.; Chen, D. S.; Lackner, M. R. *PLoS One* **2010**, *5*, e12517.

(8) Yin, C.; Wang, Y.; Ji, J.; Cai, B.; Chen, H.; Yang, Z.; Wang, K.; Luo, C.; Zhang, W.; Yuan, C.; Wang, F. *Anal chem* **2018**, *90*, 3744-3751.

(9) Li, J.; Qi, C.; Lian, Z.; Han, Q.; Wang, X.; Cai, S.; Yang, R.; Wang, C. *ACS Appl. Mater. Interfaces* **2016**, *8*, 2511-2516.

(10) Shen, Q.; Xu, L.; Zhao, L.; Wu, D.; Fan, Y.; Zhou, Y.; OuYang, W.-H.; Xu, X.; Zhang, Z.; Song, M.; Lee, T.; Garcia, M. A.; Xiong, B.; Hou, S.; Tseng, H.-R.; Fang, X. *Adv Mater* **2013**, *25*, 2368-2373.

(11) Zhao, W.; Cui, C. H.; Bose, S.; Guo, D.; Shen, C.; Wong, W. P.; Halvorsen, K.; Farokhzad, O. C.; Teo, G. S. L.; Phillips, J. A.; Dorfman, D. M.; Karnik, R.; Karp, J. M. *Proc. Natl. Acad. Sci. U.S.A.* **2012**, 19626–19631.

(12) Warkiani, M. E.; Khoo, B. L.; Wu, L.; Tay, A. K. P.; Bhagat, A. A. S.; Han, J.; Lim, C. T. *Nat Protoc* **2015**, *11*, 134-148.

(13) Park, M. H.; Reategui, E.; Li, W.; Tessier, S. N.; Wong, K. H.; Jensen, A. E.; Thapar, V.; Ting, D.; Toner, M.; Stott, S. L.; Hammond, P. T. *J Am Chem Soc* **2017**, *139*, 2741-2749.

(14) Jackson, J. M.; Witek, M. A.; Kamande, J. W.; Soper, S. A. *Chem Soc Rev* **2017**, *46*, 4245-4280.

(15) Ahmed, M. G.; Abate, M. F.; Song, Y.; Zhu, Z.; Yan, F.; Xu, Y.; Wang, X.; Li, Q.; Yang, C. *Angew Chem Int Ed Engl* **2017**, *56*, 10681-10685.

(16) Yoon, H. J.; Shanker, A.; Wang, Y.; Kozminsky, M.; Jin, Q.; Palanisamy, N.; Burness, M. L.; Azizi, E.; Simeone, D. M.; Wicha, M. S.; Kim, J.; Nagrath, S. *Adv Mater* **2016**, *28*, 4891-4897.

(17) Zheng, F.; Cheng, Y.; Wang, J.; Lu, J.; Zhang, B.; Zhao, Y.; Gu, Z. *Adv Mater* **2014**, *26*, 7333-7338.

(18) Balasubramanian, P.; Kinders, R. J.; Kummar, S.; Gupta, V.; Hasegawa, D.; Menachery, A.; Lawrence, S. M.; Wang, L.; Ferry-Galow, K.; Davis, D.; Parchment, R. E.; Tomaszewski, J. E.; Doroshow, J. H. *PLoS One* **2017**, *12*, e0175414.

(19) Vermesh, O.; Aalipour, A.; Ge, T. J.; Saenz, Y.; Guo, Y.; Alam, I. S.; Park, S.-m.; Adelson, C. N.; Mitsutake, Y.; Vilches-Moure, J.; Godoy, E.; Bachmann, M. H.; Ooi, C. C.; Lyons, J. K.; Mueller, K.; Arami, H.; Green, A.; Solomon, E. I.; Wang, S. X.; Gambhir, S. S. *Nat Biomed Eng* **2018**, *2*, 696-705.

(20) Cheng, S.-B.; Xie, M.; Xu, J.-Q.; Wang, J.; Lv, S.-W.; Guo, S.; Shu, Y.; Wang, M.; Dong, W.-G.; Huang, W.-H. *Anal Chem* **2016**, *88*, 6773-6780.

(21) Zhao, X.; Lis, J. T.; Shi, H. *Nucleic Acid Ther* **2013**, *23*, 238-242.

(22) Myung, J. H.; Eblan, M. J.; Caster, J. M.; park, s.; Poellmann, M. J.; Wang, K.; Tepper, J. E.; Tam, K. A.; Miller, S. M.; Shen, C.; Chen, R. C.; Zhang, T.; Chera, B.; Wang, A. Z.; Hong, S. *Clin Cancer Res* **2018**, *24*, 2539-2547.

(23) Zhao, W.; Ali, M. M.; Brook, M. A.; Li, Y. *Angew Chem Int Ed Engl* **2008**, *47*, 6330-6337.

(24) Fire, A.; Xu, S. Q. *Proc. Natl. Acad. Sci. U.S.A.* **1995**, *92*, 4641-4645.

(25) Ali, M. M.; Li, F.; Zhang, Z.; Zhang, K.; Kang, D. K.; Ankrum, J. A.; Le, X. C.; Zhao, W. *Chem Soc Rev* **2014**, *43*, 3324-3341.

(26) Dworzak, M. N.; Fröschl, G.; Printz, D.; Mann, G.; Pötschger, U.; Mühlegger, N.; Fritsch, G.; Gadner, H. *Blood* **2002**, *99*, 1952-1958.

(27) Sefah, K.; Tang, Z. W.; Shangguan, D. H.; Chen, H.; Lopez-Colon, D.; Li, Y.; Parekh, P.; Martin, J.; Meng, L.; Phillips, J. A.; Kim, Y. M.; Tan, W. H. *Leukemia* **2009**, *23*, 235-244.

(28) Coustan-Smith, E.; Sancho, J.; Hancock, M. L.; Razzouk, B. I.; Ribeiro, R. C.; Rivera, G. K.; Rubnitz, J. E.; Sandlund, J. T.; Pui, C. H.; Campana, D. *Blood* **2002**, *100*, 2399-2402.

(29) Papaemmanuil, E.; Gerstung, M.; Bullinger, L.; Gaidzik, V. I.; Paschka, P.; Roberts, N. D.; Potter, N. E.; Heuser, M.; Thol, F.; Bolli, N.; Gundem, G.; Van Loo, P.; Martincorena, I.; Ganly, P.; Mudie, L.; McLaren, S.; O'Meara, S.; Raine, K.; Jones, D. R.; Teague, J. W., et al. *N Engl J Med* **2016**, *374*, 2209-2221.

(30) Prebet, T.; Lhoumeau, A.-C.; Arnoulet, C.; Aulas, A.; Marchetto, S.; Audebert, S.; Puppo, F.; Chabannon, C.; Sainty, D.; Santoni, M. J.; Sebbagh, M.; Summerour, V.; Huon, Y.; Shin, W.-S.; Lee, S.-T.; Esterni, B.; Vey, N.; Borg, J.-P. *Blood* **2010**, *116*, 2315–2323.

(31) Shangguan, D.; Li, Y.; Tang, Z.; Cao, Z. C.; Chen, H. W.; Mallikaratchy, P.; Sefah, K.; Yang, C. J.; Tan, W. *Proc. Natl. Acad. Sci. U.S.A.* **2006**, *103*, 11838-11843.

(32) Sheng, W.; Chen, T.; Tan, W.; Fan, Z. H. *ACS Nano* **2013**, *7*, 7067-7076.

(33) Mallikaratchy, P. R.; Ruggiero, A.; Gardner, J. R.; Kuryavyi, V.; Maguire, W. F.; Heaney, M. L.; McDevitt, M. R.; Patel, D. J.; Scheinberg, D. A. *Nucleic Acids Res* **2011**, *39*, 2458-2469.

(34) Vorobyeva, M.; Vorobjev, P.; Venyaminova, A. *Molecules* **2016**, *21*, 1613.

(35) Prins., A. V. R. A. M. D. J. M. W. J. *15th International Conference on Miniaturized Systems for Chemistry and Life Sciences, Seattle, Washington, USA* **2011**, *117*, 1627–1629.

(36) van Reenen, A.; de Jong, A. M.; Prins, M. W. J. *J Phys Chem B* **2013**, *117*, 1210-1218.

(37) Truhlar, D. G. *J Chem Educ* **1985**, *62*, 104-106.

(38) Porciani, D.; Cardwell, L. N.; Tawiah, K. D.; Alam, K. K.; Lange, M. J.; Daniels, M. A.; Burke, D. H. *Nat Commun* **2018**, *9*, 2283.

(39) Foged, C.; Brodin, B.; Frokjaer, S.; Sundblad, A. *Int J Pharm* **2005**, *298*, 315-322.

(40) Huang, C.-C.; Liao, Z.-X.; Lu, H.-M.; Pan, W.-Y.; Wan, W.-L.; Chen, C.-C.; Sung, H.-W. *Chem Mater* **2016**, *28*, 9017-9025.

(41) Bakthavathsalam, P.; Longatte, G.; Jensen, S. O.; Manefield, M.; Gooding, J. J. *Sensor Actual B-Chem* **2018**, *268*, 255-263.

(42) Obika, S.; Nanbu, D.; Hari, Y.; Andoh, J.-i.; Morio, K.-i.; Doi, T.; Imanishi, T. *Tetrahedron Lett* **1998**, *39*, 5401-5404.

(43) Zhao, W.; Brook, M. A.; Li, Y. *Methods Mol Biol* **2008**, *474*, 79-90.

(44) Adalsteinsson, B. T.; Gudnason, H.; Aspelund, T.; Harris, T. B.; Launer, L. J.; Eiriksdottir, G.; Smith, A. V.; Gudnason, V. *PLoS One* **2012**, *7*, e46705.

Authors are required to submit a graphic entry for the Table of Contents (TOC) that, in conjunction with the manuscript title, should give the reader a representative idea of one of the following: A key structure, reaction, equation, concept, or theorem, etc., that is discussed in the manuscript. Consult the journal's Instructions for Authors for TOC graphic specifications.

Insert Table of Contents artwork here